Electrochemical, Magnetic, and Electrical Properties of α,ω-Capped Sexithiophene Films. Part 3. Conduction in Poly(bis-terthienyl-B)s (B = Ethane, Disulfide, Diacetylene, Acetylene, Ethylene)

G. Zotti,*[,†] B. Vercelli,[†] A. Berlin,*[,‡] S. Destri,[§] M. Pasini,[§] V. Hernández,[||] and J.T. López Navarrete[||]

Istituto CNR per l′ Energetica e le Interfasi, c.o Stati Uniti 4, 35127 Padova, Italy, Istituto CNR di Scienze e Tecnologie Molecolari, via C. Golgi 19, 20133 Milano, Italy, Istituto CNR per lo Studio delle Macromolecole, via E. Bassini 15, 20133 Milano, Italy, and Departamento de Química Física, Universidad de Málaga, 29071 Málaga, Spain

Received June 11, 2008. Revised Manuscript Received September 16, 2008

Electrochemical oxidation of bis-terthienyl-B (B = ethane, disulfide, diacetylene, acetylene, ethylene) has been investigated. Monomers without and with 3,3″-dialkylsubstitution are regularly coupled to polymers alternating sexithiophene and B moieties. The corresponding terthienyl homopolymers have also been produced for comparison. The polymers obtained are characterized by cyclic voltammetry, EQCM, UV−vis, and FTIR spectroscopy, in situ ESR and in situ conductivity. The conductivities of p-doped polymers with ethane or disulfide bridges fall in a narrow range ($1-5 \times 10^{-2}$ S cm^{-1}) and are practically the same as those of α,ω-dimethylsexithiophene (1×10^{-2} S cm^{-1}), suggesting that conduction proceeds without the help of the links via a direct redox hopping between sexithiophene blocks of adjacent polymer chains. In the cases of diacetylene and acetylene, conduction changes from redox to bipolaron-type but only in the case of ethylene the conductivity jumps to high values ($1-5$ S cm^{-1}) corresponding to those of the polymers without the bridging moiety B, i.e., with shortened thiophene rings. DFT calculations of the bridge energy levels account for this result.

1. Introduction

Carrier mobility in polyconjugated materials is the basic issue for the production of efficient optoelectronic organic devices such as light emitting diodes, field-effect transistors, and solar cells.[1] In particular, the polythiophene system has been mostly addressed for application in organic field-effect transistors (OFETs)[2] and photovoltaic diodes (PVs).[3] It has been found that mobility increases as the conjugation length is increased up to 14 thiophene rings.[4] In any case, sexithiophene, which is peculiar because its conductivity is redox-type [5,6] vs the metal-like conductivity of higher oligomers,[7] is the object of by far the major amount of research.

Scheme 1

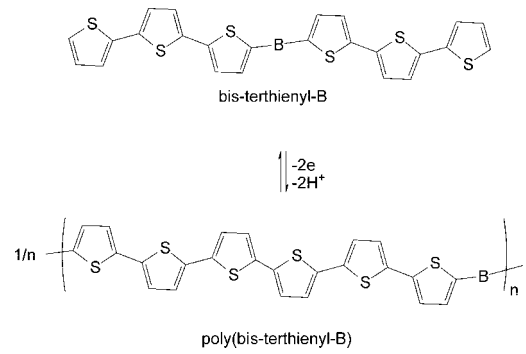

In Parts 1 and 2 of this series,[6,7] we have investigated the conductive properties of sexithiophenes capped with different moieties. We have now considered that the sexithiophene moiety may also be part of regular polymers produced by anodic coupling of bis-terthiophene-B monomers, where B is a generic symmetrical moiety bridging the two terthiophene ends (see Scheme 1). In such polymers, a conductive contribution may come also from transport within the polymer chain, a matter recently considered on a theoretical basis right for oligo- and polythiophenes.[8]

To establish the contribution of such intrachain lateral (through-bridge) vs interchain parallel (face-to-face) conduction in such poly(sexithiophene-bridge)s, we have modulated both the conjugation degree of the bridge from disulfide to

* Corresponding author. Tel: (39)49-8295868. Fax: (39)49-8295853. E-mail: g.zotti@ieni.cnr.it.
† Istituto CNR per l′ Energetica e le Interfasi.
‡ Istituto CNR di Scienze e Tecnologie Molecolari.
§ Istituto CNR per lo Studio delle Macromolecole.
|| Universidad de Málaga.

(1) Walzer, K.; Maennig, B.; Pfeiffer, M.; Leo, K. *Chem. Rev.* **2007**, *107*, 1233.
(2) (a) Kline, R. J.; McGehee, M. D.; Kadnikova, E. N.; Liu, J.; Frechet, J. M. J. *Adv. Mater.* **2003**, *15*, 1519. (b) Ong, B. S.; Wu, Y.; Liu, P.; Gardner, S. *J. Am. Chem. Soc.* **2004**, *126*, 3378.
(3) Li, G.; Shrotriya, V.; Huang, J.; Yao, Y.; Moriarty, T.; Emery, K.; Yang, Y. *Nat. Mater.* **2005**, 864.
(4) Harima, Y.; Kim, D.-H.; Tsutitori, Y.; Jiang, X.; Patil, R.; Ooyama, Y.; Ohshita, J.; Kunai, A. *Chem. Phys. Lett.* **2006**, *420*, 387.
(5) Zotti, G.; Schiavon, G.; Berlin, A.; Pagani, G. *Adv. Mater.* **1993**, *5*, 551.
(6) Zotti, G.; Zecchin, S.; Vercelli, B.; Berlin, A.; Grimoldi, S.; Pasini, M. C.; Raposo, M. M. M. *Chem. Mater.* **2005**, *17*, 6492.
(7) Zotti, G.; Zecchin, S.; Vercelli, B.; Pasini, M.; Destri, S.; Bertini, F.; Berlin, A. *Chem. Mater.* **2006**, *18*, 3151.
(8) Lacroix, J. C.; Chane-ChingK.I.; Maquere, F.; Maurel, F. *J. Am. Chem. Soc.* **2006**, *128*, 7264.

10.1021/cm8023007 CCC: $40.75
Published on Web 10/21/2008

Scheme 2

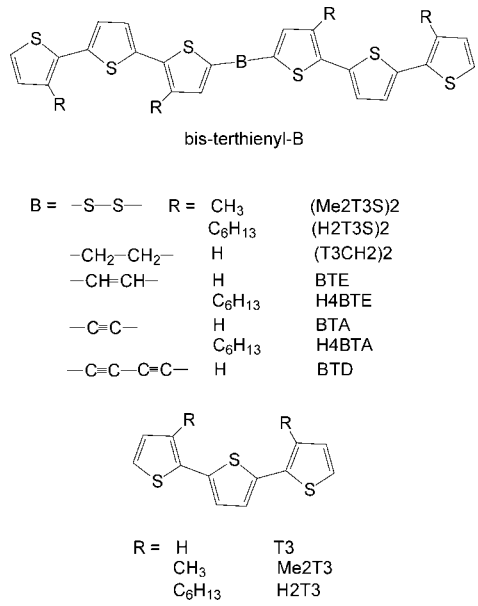

diacetylene through acetylene and ethylene moieties and varied the spacing among chains by methyl- and hexyl-substitution at the thienyl rings. To this end, we have synthesized and electropolymerized the monomers shown in Scheme 2.

Anodic coupling of the alkane-bridged bis-terthienylethane has been previously performed[9] and the corresponding polymer with tetrahexyl-substituted sexithiophene moieties has been subsequently produced via reductive coupling.[10] Both the nonsubstituted[9] and the alkyl-substituted[11] polymers have undergone potential-controlled conductivity investigations. We have here considered the disulfide as the bridge connecting sexithiophene moieties in a polymer for a possible participation of the electron-rich S−S moiety to the conjugated path. A polybithiophene bearing disulfide linkers has in fact been previously produced[12] but in that case the disulfide were bond in the 3-positions. These novel cross-linked electroactive polymers attained electrical conductivity of 0.04 S cm^{-1} upon iodine doping. Electrochemistry of diaryl-disulfides has clarified that oxidation in aprotic media produces first the S−S localized dication (see B in Scheme 3).[13] This result is suggesting that delocalization over a longer conjugated chain such as sexithiophene may stabilize the dicationic form.

Inserting an ethylene moiety between thiophene[14] or bithiophene[15] units leads to polymers with high conductivities, whereas terthiophenes originate monomers that stabilize

Scheme 3

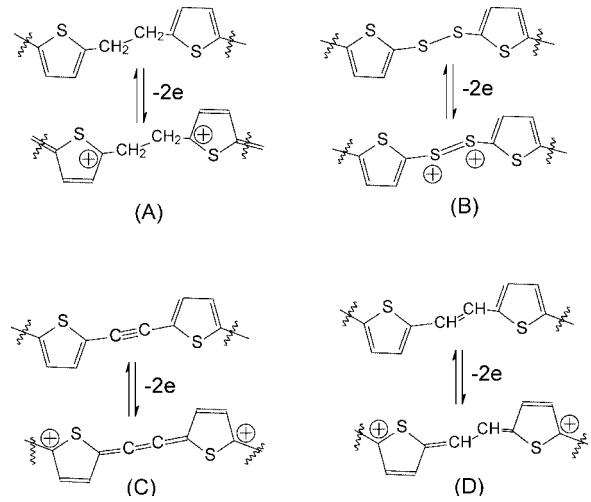

the radical cation form.[16] Thus the double bond apparently eases the electrical connection between the thiophene units.

The insertion of ethynyl groups between oligothiophene units has allowed in the past the production of a series of polymers.[17−21] The insertion of diacetylene moieties is far more limited. Recently, cyclic oligothiophene-diacetylenes were produced,[20] and among these, those bearing terthiophene are the most investigated. Dithienyl-diacetylenes are also been reported and electropolymerized.[21]

In this paper, we report the synthesis and electropolymerization of the monomers shown in Scheme 2, the characterization of the produced polymers by cyclic voltammetry, EQCM, ESR, UV−vis and FTIR spectroscopy, and in situ ESR. A detailed investigation of their conductive properties by in situ conductivity techniques, supported by DFT calculations, constitutes the core part of this investigation, the third in the series.

2. Experimental and Computational Details

2.1. Chemicals and Reagents. All reactions of air- and water-sensitive materials were performed under nitrogen. Air- and water-sensitive solutions were transferred with double-ended needles. The solvents used in the reactions (Fluka) were absolute and stored over molecular sieves. Acetonitrile was reagent grade (Uvasol, Merck)

(9) Berlin, A.; Fontana, G.; Pagani, G.; Schiavon, G.; Zotti, G. *Synth. Met.* **1993**, *55−57*, 4796.
(10) Sato, M. A.; Sakamoto, M. A.; Miwa, M.; Hiroi, M. *Polymer* **2000**, *41*, 5681.
(11) Jiang, X.; Harima, Y.; Zhu, L.; Kunugi, Y.; Yamashita, K.; Sakamoto, M. A.; Sato, M. A. *J. Mater. Chem.* **2001**, *11*, 3043.
(12) Ng, S. C.; Miao, P. *Macromol. Chem. Phys.* **1999**, *200*, 2166.
(13) Boryczka, S.; Elothmani, D.; Do, Q. T.; Simonet, J.; LeGuillanton, G. *J. Electrochem. Soc.* **1996**, *143*, 4027.
(14) Bragadin, M.; Cescon, P.; Berlin, A.; Sannicolo, F. *Makromol. Chem.* **1987**, *188*, 1425.
(15) Berlin, A.; Zotti, G. *Synth. Met.* **1999**, *106*, 197.
(16) Casado, J.; Miller, L. L.; Mann, K. R.; Pappenfus, T. M.; Kanemitsu, Y.; Orti, E.; Viruela, P. M.; Pou-Amerigo, R.; Hernandez, V.; Lopez Navarrete, J. T. *J. Phys. Chem. B* **2002**, *106*, 3872.
(17) Yamamoto, T.; Yamada, W.; Takagi, M.; Kizu, K.; Maruyama, T.; Ooba, N.; Tomaru, S.; Kurihara, T.; Kaino, T.; Kubota, K. *Macromolecules* **1994**, *27*, 6620, and references therein.
(18) Sirringhaus, H.; Brown, P. J.; Friend, R. H.; Nielsen, M. M.; Bechgaard, K.; Langeveld-Voss, B. M. W.; Spiering, A. J. H.; Janssen, R. A. J.; Meijer, E. W.; Herwig, P.; de Leeuw, D. M. *Nature* **1999**, *401*, 685.
(19) (a) Tormos, G. V.; Nugara, P. N.; Lakshmikantham, M. V.; Cava, M. P. *Synth. Met.* **1993**, *53*, 271. (b) Chimenti, F.; D'Ilario, L.; Ettorre, A.; Muraglia, E.; Ortaggi, G.; Sleiter, G. *J. Mater. Sci. Lett.* **1992**, *11*, 1532. (c) Kossmehl, G. *Makromol. Chem. Macromol. Symp.* **1986**, *4*, 45. (d) Ng, S. C.; Chan, H. S. O.; Leong, L. S.; Sarkar, A. *J. Mater. Sci. Lett.* **1996**, *15*, 664. (e) Pearson, D. L.; Schumm, J. S.; Tour, J. M. *Macromolecules* **1994**, *29*, 2348. (f) Zotti, G.; Schiavon, G.; Zecchin, S. M.; Berlin, A. *Synth. Met.* **1998**, *97/3*, 245.
(20) Krömer, J.; Rios-Carreras, I.; Fuhrmann, G.; Musch, C.; Wunderlin, M.; Debaerdemaeker, T.; Mena-Osteritz, E.; Bäuerle, P. *Angew. Chem., Int. Ed.* **2000**, *39*, 3481.
(21) Sarkar, A.; Talwar, S.; Okada, S.; Nakanishi, H. *Polym. Bull.* **1999**, *42*, 69.

with a water content <0.01%. The supporting electrolyte tetrabutylammonium perchlorate (Bu_4NClO_4) and all other chemicals used for characterizations were reagent grade and used as received.

The compounds 5-bromo-2,2′:5′,2″-terthiophene,[22] 3′,3″-dihexyl-2,2′:5′,2″-terthiophene (H2T3),[23] 5-bromo-3,3″-dihexyl-2,2′:5′,2″-terthiophene,[24] 3,3″-dihexyl-2,2′:5′,2”-terthiophene-5-carbaldehyde,[23] bis(3,3″-dimethyl-2,2′:5′,2″-terthiophen-5-yl) disulfide [(Me2T3S)2],[25] bis(3,3″-dihexyl-2,2′:5′,2″-terthiophen-5-yl) disulfide [(H2T3S)2],[25] (*E*)-1,2-bis(2,2′:5′,2″-terthiophene-5-yl)ethylene (BTE),[26] and 5-ethynyl-2,2′:5′5″-terthiophene[27] were prepared as described in the literature. The compound (*E*)-1,2-Bis(3,3″-dihexyl-2,2′:5′,2″-terthiophene-5-yl)ethylene (H4BTE) was prepared following the same procedure described in the literature[26] for the unsubstituted compound BTE, as reported below. 1,4-Bis[2-(2,2′:5′5″-terthienyl)diacetylene (BTD), 1,2-bis(2,2′;5′,2″-terthienyl-5-yl)acetylene (BTA), and 1,2-bis(3,3″-dihexyl-2,2′:5′,2″-terthienyl-5-yl)acetylene (H4BTA) were produced as reported below.

^{1}H and ^{13}C NMR spectra were recorded on a Bruker FT 300 (300 MHz for ^{1}H); chemical shift values are given in parts per million. Electron-impact mass spectrometry measurements were performed on a VG ZAB-2F spectrometer equipped with an FI/FD ion source. Matrix-assisted laser desorption ionization (MALDI) mass spectra were obtained by an Ultraflex II mass spectrometer (Bruker Daltonics) operating both in the positive reflectron and in the linear modes, using 2,5-dihydroxybenzoic acid as the matrix.

*(*E*)-1,2-Bis(3,3″-dihexyl-2,2′:5′,2″-terthiophene-5-yl)ethylene (H4BTE).* $TiCl_4$ (1.05 mL of a 1 M solution in CH_2Cl_2) was added dropwise to a stirred solution of 3,3″-dihexyl-2,2′:5′,2”-terthiophene-5-carbaldehyde (155 mg, 0.34 mmol) in THF (10 mL), keeping the temperature at −18 °C. Zn powder (137 mg, 2.10 mmol) was added portionwise. After 0.5 h of stirring, the reaction mixture was refluxed for 3 h. Water was added and the mixture extracted with CH_2Cl_2; the organic phase was was dried (Na_2SO_4), and the solvent evaporated. Flash chromatography of the residue (silica gel, hexane) afforded the title compound (95 mg, 65% yield). HREIMS: calcd, 856.3332; found, 856.3329. Anal. Calcd for $C_{50}H_{64}S_6$: C, 70.04; H, 7.52%. Found: C, 69.92; H, 7.37%. ^{1}H NMR ($CDCl_3$): δ 0.89 (m, 12H), 1.35 (m, 24H), 1.65 (m, 8H), 2.75 (t, 4H), 2.79 (t, 4H), 6.86 (s, 2H), 6.90 (s, 2H), 6.93 (d, 2H), 7.06 (m, 4H), 7.17 (d, 2H). ^{13}C NMR ($CDCl_3$): δ 14.06, 22.61, 29.24, 29.33, 29.48, 30.40, 30.69, 31.69, 121.20, 123.79, 125.81, 126.13, 126.54, 129.58, 130.08, 130.38, 136.11, 139.78, 140.10. IR: ν_{max} CH out-of-plane deformation, 930 cm^{-1}. The (*E*)-isomer was assigned from its IR spectrum and from the fact that the reductive coupling reaction of thiophene-2-carbaldehydes promoted by low-valence titanium[26] gives almost exclusively the (*E*)-isomer.

1,4-Bis[2-(2,2′:5′5″-terthienyl)diacetylene (BTD). The symmetrical coupling using Glaser reaction of terminal acetylene molecules provided the above product in high yields. The starting 5-ethynyl-2,2′:5′5″-terthiophene (272 mg, 1.0 mmol) was added to a mixture of $CuCl_2$ (60 mg, 0.3 mmol) and *N*,*N*,*N*′,*N*′-tetramethylethylendiamine (0.2 mL) in 20 mL of dimethoxyethane. The mixture was heated at 35 °C for 2 h while dry air was bubbled through and then poured into water. The resulting precipitate was filtered off, washed with water, dried, and recrystallized from dioxane to yield the title product (248 mg, 85% yield) Mp. 253−254 °C; MS *m*/*e* 542 [M$^+$]. FTIR (cm^{-1}): 3067 (aromatic C−H stretching), 2185 (C'C stretching) 1465 (C−C thiophene stretching), 794 (inner thiophene ring bending). Anal. Calcd for $C_{28}H_{14}S_6$ C, 61.99; H, 2.58; S, 35.42%. Found: C, 62.03; H, 3.5; S, 34.47%. ^{1}H NMR (deuterated TCE, 72 °C): δ 7.19 (br, 2H); 7.13 (br, 1H); 7.05 (br, 1H); 7.02 (br, 1H); 6.97 (br, 2H). ^{13}C NMR (deuterated TCE, ppm): δ 138.39, 135.71, 135.71, 134.70, 133.67, 133.05, 126.08, 123.57, 123.18, 122.67, 122.36, 121.66, 118.54, 77.49, 65.08.

1,2-Bis(3,3″-dihexyl-2,2′:5′,2″-terthienyl-5-yl)acetylene (H4BTA). To a degassed solution of 5-bromo-3,3″-dihexyl-2,2′:5′,2″-terthiophene (165 mg, 0.33 mmol) was added bis(tributylstannyl)acetylene (96.6 mg, 0.16 mmol) in dry toluene (5 mL) $Pd(PPh_3)_4$ (7 mg, 0.006 mmol). The mixture was heated at 80 °C under nitrogen. After 24 h, the reaction mixture was cooled to room temperature, the solvent was removed, and the residue was purified by flash column chromatography (silica gel, hexane/dichloromethane 7/3) to provide the title product as an orange solid (yield 63%). Mp: 40−43. MS (EI), *m*/*e*: 856 (M$^{\bullet+}$). FTIR (cm^{-1}): 3067 (aromatic C−H stretching), 2924 (aliphatic C−H stretching), 2182 (C−C stretching), 1465 (C−C thiophene stretching), 794 (inner thiophene ring bending). Anal. Calcd for $C_{50}H_{62}S_6$: C, 70.19; H, 7.33; S, 22.48%. Found: C, 71.02; H, 6.9; S, 22.08%. ^{1}H NMR ($CDCl_3$): δ 7.2 (d, 2H, J = 5.2), 7.13 (s, 2H), 7.15 (d, 2H, J = 3.8), 7.1 (d, 2H, J = 3.8), 6.9 (d, 2H, J = 5.2), 2.73, (m, 8H), 1.63, (m, 8H), 1.4 (m, 8H), 1.3 (br, 16H), 0.88 (m, 12H).

^{13}C NMR ($CDCl_3$): δ 139.88, 139.55, 136.52, 135.25, 134.74, 132.71, 130.22, 129.93, 126.34, 125.99, 123.93120.07, 87.35, 31.56, 30.55, 30.31, 29.28, 29.16, 29.09, 22.55, 14.1.

1,2-Bis(2,2′;5′,2″-terthienyl-5-yl)acetylene (BTA). To a degassed solution of 5-bromo-2,2′;5′,2″-terthiophene (100 mg, 0.3 mmol) was added bis(tributylstannyl)acetylene (78.9 mg, 0.13 mmol) in dry toluene (5 mL), $Pd(PPh_3)_4$ (7 mg, 0.006 mmol). The mixture was heated at 80 °C under nitrogen. After 24 h, the reaction mixture was cooled to room temperature and filtered, and the solid was washed with cold toluene to give the pure title compound as a dark orange solid (57% yield), mp >200 °C (with decomposition) MS(EI), *m*/*e*: 516 (M•+).

FTIR (cm^{-1}): 3067 (aromatic C−H stretching), 2185 (C−C stretching) 1465 (C−C thiophene stretching), 794 (inner thiophene ring bending). Anal. Calcd for $C_{26}H_{14}S_6$ C, 60.23; H, 2.7; S, 37.06%. Found: C, 61.4; H, 3.1; S, 35.5%. ^{1}H NMR (deuterated TCE 103 °C): δ 7.16 (d br, 1H), 7.11 (br, 2H), 7.01 (br, 2H), 6.98 (d, 1H, J = 4.3), 6.94, (dd, 1H, J = 4.3, J = 3.7).

Electrosynthesis of H4BTE Dimer. Bulk H4BTE dimer has been produced by exhaustive electrolysis (ca. 2 F mol^{-1}) at 0.45 V of 10 mg H4BTE in 25 mL CH_2Cl_2 + 0.1 M Bu_4NClO_4. The dark suspension of the oxidized products was left to react overnight and then reduced to a red-orange solution with a few drops of hydrazine in 2 mL of acetonitrile (λ_{max} in $CHCl_3$ = 465 nm). The solution was then evaporated, washed with acetonitrile (to remove supporting electrolyte, unreacted monomer, and side products), and dried (yield: 90%). MS (MALDI) [M+H]$^+$ *m/e:* 1714.

2.2. Apparatus and Procedure. *Electrochemistry and Spectroscopy.* Experiments were performed at room temperature under nitrogen in three-electrode cells using 0.1 M Bu_4NClO_4 as supporting electrolyte. The counter electrode was platinum; the reference electrode was a silver/0.1 M silver perchlorate in acetonitrile (0.34 V vs SCE). The voltammetric apparatus (AMEL, Italy) included a 551 potentiostat modulated by a 568 programmable function generator and coupled to a 731 digital integrator.

The working electrode for cyclic voltammetry was a platinum minidisc electrode (0.003 cm^2). For electronic spectroscopy, a 0.8 × 2.5 cm indium−tin-oxide (ITO) sheet (ca. 20 ohm/square resistance, from Balzers, Liechtenstein) was used.

(22) Bauerle, P.; Wuerthner, F.; Goetz, G.; Effenberger, F. *Synthesis* **1993**, 1099.
(23) Jones, C. L.; Higging, S. J. *J. Mater. Chem.* **1999**, *9*, 865.
(24) Destri, S.; Ferro, D. R.; Khotina, I. A.; Porzio, W.; Farina, A. *Macromol. Chem. Phys.* **1998**, *1999*, 1973.
(25) Zotti, G.; Vercelli, B.; Berlin, A. *Chem. Mater.* **2008**, *20*, 397.
(26) Nakayama, J.; Murabayashi, S.; Hoshino, M. *Heterocycles* **1986**, *24*, 2639.
(27) Kagan, J.; Arora, S. K. *J. Org. Chem.* **1983**, *48*, 4317.

Electronic spectra were obtained from a Perkin-Elmer Lambda 15 spectrometer; FTIR spectra were taken on a Perkin-Elmer 2000 FTIR spectrometer. FTIR spectra of films were taken in reflection−absorption mode.

EQCM. Electrochemical quartz crystal microbalance (EQCM) analysis was performed with a platinum-coated AT-cut quartz electrode (0.2 cm^2), resonating at 9 MHz, onto which the polymers were deposited. The oscillator circuit was homemade and the frequency counter was Hewlett-Packard mod.5316B. Data were collected by a microcomputer with a homemade analyzing software by which frequency changes were monitored as mass changes Δm. The dry mass and charge measurements were performed according to the procedure previously published.[28]

ESR. ESR spectra were taken on a Bruker ER 100D following the procedure previously described.[29] Absolute spin calibration was performed with $VOSO_4 \cdot 5H_2O$ crystals, *g*-value calibration with thin films of DPPH ($g = 2.0036$ [30]).

Conductivity. The apparatus and procedures used for conductivity experiments were previously described in detail.[31,32] The electrode was typically a two-band platinum electrode (0.3 cm × 0.01 cm for each band) with interband spacing of 20 μm. In the case of conductivities lower than 1×10^{-2} S cm^{-1}, the electrode was a microband array platinum electrode (5 μm bandwidth, 100 nm thick) with interband spacing of 5 μm. The deposit was thick enough to ensure minimum resistance, under which condition the conductivity σ is given by $\sigma = k/(R - R_0)$, where R is the measured resistance, R_0 the lead resistance, and k the cell constant.

2.3. Quantum Chemical Calculations. Density functional theory (DFT) calculations were carried out using the Gaussian 03 program[33] running on SGI Origin supercomputer. Becke's three-parameter exchange functional combined with the LYP correlation functional (B3LYP)[34] was employed, because it has been shown that the B3LYP functional yields similar geometries for medium-sized molecules as those obtained from the MP2 calculations with the same basis sets.[35] The standard 6−31G** basis set was used to obtain optimized geometries on isolated entities.[36] Vertical electronic excitation energies were computed by using the time-dependent DFT (TDDFT) approach[37,38] on v previously optimized molecular geometries.

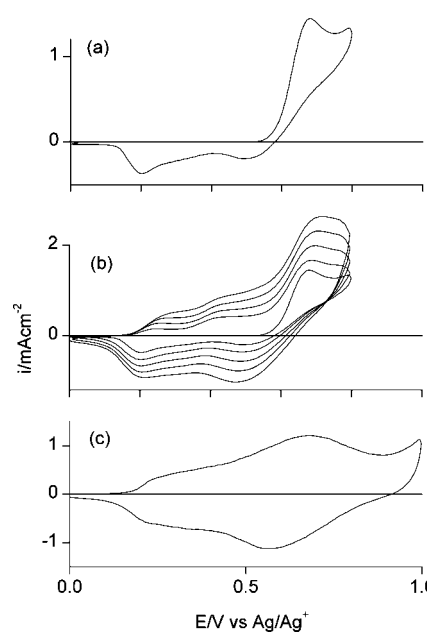

Figure 1. (a) Single and (b) repetitive cyclic voltammogram of (Me2T3S)2 1×10^{-3} M in CH_2Cl_2 + 0.1 M Bu_4NClO_4; (c) cyclic voltammogram of poly(Me2T3S)2 film in CH_2Cl_2 + 0.1 M Bu_4NClO_4. Scan rate: 0.1 V s^{-1}.

3. Results and Discussion

3.1. Electrochemical Polymerization and Analysis. Cyclic voltammetry (CV) of the monomers was typically performed in 1×10^{-3} M solutions in CH_2Cl_2 at room temperature (for alkylsubstituted monomers such as (Me2T3S)2, (H2T3S)2, H4BTA, and H4BTE) or chlorobenzene at 50 °C (for non alkylated monomers such as BTD, BTA and BTE, due to their scarce solubility). The CV (Figure 1a) shows an irreversible oxidation of the monomer (peak potentials are summarized in Table 1) and repetitive scans produce in general an increase in the CV response (Figure 1b) as indication of polymer electrodeposition (BTE-based monomers behave differently, see below). According to the usual mechanism of coupling, the oxidation product is in fact the α-coupled polymer, as illustrated in Scheme 1, and the analytical results reported below agree with this formulation. The polymer films produced in this way are subsequently investigated in acetonitrile and the obtained redox potentials are also summarized in Table 1.

We have previously reported[9] that the cyclic voltammetry of bis-terthienyl-ethane (T3CH2)2 (see Scheme 1) shows an irreversible oxidative peak at 0.7 V with the build up of a reversible process similar to that displayed by sexithiophene

(28) Zotti, G.; Zecchin, S.; Schiavon, G.; Groenendaal, L. *Chem. Mater.* **2000**, *12*, 2996.
(29) Zotti, G.; Schiavon, G. *Synth. Met.* **1989**, *31*, 347.
(30) Inzelt, G.; Day, R. W.; Kinstle, J. F.; Chambers, J. Q. *J. Phys. Chem.* **1983**, *87*, 4592.
(31) Schiavon, G.; Sitran, S.; Zotti, G. *Synth. Met.* **1989**, *32*, 209.
(32) Aubert, P. H.; Groenendaal, L.; Louwet, F.; Lutsen, L.; Vanderzande, D.; Zotti, G. *Synth. Met.* **2002**, *126*, 193.
(33) Frisch, M. J.; Trucks, G. W.; Schlegel, H. B.; Scuseria, G. E.; Robb, M. A.; Cheeseman, J. R.; Montgomery, J. A. Jr.; Vreven, T.; Kudin, K. N.; Burant, J. C.; Millam, J. M.; Iyengar, S. S.; Tomasi, J.; Barone, V.; Mennucci, B.; Cossi, M.; Scalmani, G.; Rega, N.; Petersson, G. A.; Nakatsuji, H.; Hada, M.; Ehara, M.; Toyota, K.; Fukuda, R.; Hasegawa, J.; Ishida, M.; Nakajima, T.; Honda, Y.; Kitao, O.; Nakai, H.; Klene, M.; Li, X.; Knox, J. E.; Hratchian, H. P.; Cross, J. B.; Adamo, C.; Jaramillo, J.; Gomperts, R.; Stratmann, R. E.; Yazyev, O.; Austin, A. J.; Cammi, R.; Pomelli, C.; Ochterski, J. W.; Ayala, P. Y.; Morokuma, K.; Voth, G. A.; Salvador, P.; Dannenberg, J. J.; Zakrzewski, V. G.; Dapprich, S.; Daniels, A. D.; Strain, M. C.; Farkas, O.; Malick, D. K.; Rabuck, A. D.; Raghavachari, K.; Foresman, J. B.; Ortiz, J. V.; Cui, Q.; Baboul, A. G.; Clifford, S.; Cioslowski, J.; Stefanov, B. B.; Liu, G.; Liashenko, A.; Piskorz, P.; Komaromi, I.; Martin, R. L.; Fox, D. J.; Keith, T.; AlLaham, M. A.; Peng, C. Y.; Nanayakkara, A.; Challacombe, M.; Gill, P. M. W.; Johnson, B.; Chen, W.; Wong, M. W.; Gonzalez, C.; Pople, J. A. *Gaussian 03*, revision B.04; Gaussian Inc.: Pittsburgh, PA, 2003.
(34) Becke, A. D. *J. Chem. Phys.* **1993**, *98*, 1372.
(35) Stephens, P. J.; Devlin, F. J.; Chabalowski, F. C. F.; Frisch, M. J. *J. Phys. Chem.* **1994**, *98*, 11623.
(36) Francl, M. M.; Pietro, W. J.; Hehre, W. J.; Binkley, J. S.; Gordon, M. S.; Defrees, D. J.; Pople, J. A. *J. Chem. Phys.* **1982**, *77*, 3654.
(37) (a) Runge, E.; Gross, E. K. U. *Phys. Rev. Lett.* **1984**, *52*, 997. (b) Gross, E. K. U.; Kohn, W. *Adv. Quantum Chem.* **1990**, *21*, 255. (c) Gross, E. K. U.; Ullrich, C. A.; Gossman, U. J.; *Density Functional Theory* ; Gross, E. K. U., Driezler, R. M., Eds.; Plenum Press: New York, 1995.
(38) Koch, W.; Holthausen, M. C. *A Chemist's Guide to Density Functional Theory*; Wiley-VCH: Weinheim, Germany, 2000.
(39) Zotti, G.; Schiavon, G.; Berlin, A.; Pagani, G. *Chem. Mater.* **1993**, *5*, 620.

Table 1. Monomer Oxidation Peak Potentials (E_{pm}) and Absorption (λ_m) and Polymer[a] Oxidation Redox Potentials (E^0_p), Adsorption (λ_p), and Conductivity (σ)

monomer	E_{pm} (V)	E^0_p (V)	λ_m (nm)[b]	λ_p (nm)	σ (S cm^{-1})
(T3CH2)2 [9]	0.70				5×10^{-3}
(Me2T3S)2	0.65	0.25; 0.65	370	462	2×10^{-2}
(H2T3S)2	0.65	0.53; 0.67	357	442	1×10^{-2}
BTA	0.70	0.50	401	450	2×10^{-2}
H4BTA	0.67	0.37; 0.60	405	474	5×10^{-2}
BTD	0.78	0.55; 0.80	434	475	2×10^{-2}
BTE	0.40[c];0.57[d]	0.27; 0.53	465	500	
H4BTE	0.37[c];0.53[c]	0.20; 0.50	440	510	1−5
α-MeT3[5,39]	0.70	0.50; 0.72	360	445[d]	1×10^{-2}
T3[48]	0.71	0.15	355	507	1.5
Me2T3	0.65	0.15	342	500	1
H2T3	0.65	0.20	339	532	50

[a] Dimer α,ω-dimethylsexithiophene for α-MeT3. [b] In chloroform. [c] E^0. [d] In chlorobenzene.

T6 and due to a poly(sexithiophene) film. The behavior of most of the investigated polymer films reported below is similar.

The CV of the polymer films from (Me2T3S)2 and (H2T3S)2 shows two redox processes (Figure 1c). It is worth noting that the CV of these polymers does not show any sign of capacitive behavior at full oxidation, therefore anticipating the insulating nature of the two-electron oxidation state evidenced by the conductivity measurements given below.

The oxidation redox process of poly(BTD) is also in this case a round twin and reversible response. After the results obtained for α,ω-dimethylsexithiophene,[39] the process corresponds to an overall two-electron oxidation of the sexithiophene moieties, as confirmed by EQCM (see below).

It is interesting to note (see Table 1) that the oxidative redox potentials of poly(BTD) are practically the same as those of α,ω-dimethylsexithiophene, which may be accounted for by the compensation of a lower electron donation and a higher conjugation of the triple bonds.

The behavior of poly(BTA) and poly(H4BTA) deposits are similar. The reversible oxidation processes of the polymers occur at potentials less positive than for poly(BTD) because of a reduced electronwithdrawing ability of the single acetylene moiety.

Differently from the disulfide-bridged polymers, the CVs of all these polymers do show a clear capacitive behavior at full oxidation, therefore revealing a conductive state after the two-electron oxidation. This indication has been confirmed by the conductivity measurements reported below.

BTE-Based Monomers. The cyclic voltammograms of monomers BTE and H4BTE (Figure 2a) are distinguished from the others since they show two reversible oxidation processes where CV cycling does not produce polymer film deposition. This result indicates full delocalization of the unpaired electron in the radical cation over the six thiophene rings and the connecting ethylene bridge, which makes it stable on the CV time scale (but not for hours, see below). Instead polymerization on the electrode surface occurs at higher potentials (1.1 V, Figure 2b) where further oxidation to radical trication causes fast polymerization, as previously observed in oligopyrroles[40] and oligofluorenes.[41] For H4BTE,

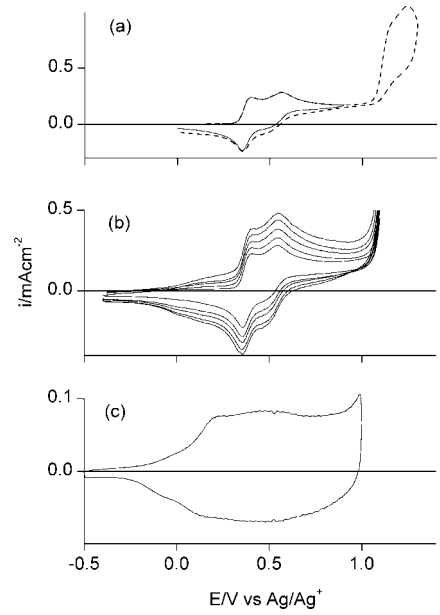

Figure 2. (a) Single CV scans at two switching potentials and (b) repetitive CV scans at high switching potential of H4BTE 1×10^{-3} M in 1:1 acetonitrile/CH_2Cl_2 + 0.1 M Bu_4NClO_4; (c) cyclic voltammogram of poly(H4BTE) film in acetonitrile + 0.1 M Bu_4NClO_4. Scan rate: 0.1 V s^{-1}.

this fact occurs in a 1:1 acetonitrile:CH_2Cl_2 mixture because in CH_2Cl_2 alone the higher solubility prevents precipitation of the polymer formed at the trication level of oxidation.

The polymer deposits show in acetonitrile a twin oxidation redox process (Figure 2c) at less positive potentials than for the monomer films. The CV shows clear capacitive features at the positive potential limit.

Bulk H4BTE dimer has been obtained oxidizing the monomer in CH_2Cl_2 solution to the radical cation and then leaving it to dimerize overnight (see Experimental Section). The product is a red solid, soluble in $CHCl_3$, for which mass spectroscopy has confirmed the dimeric formulation. Its CV is similar with that of the polymer produced by CV (in fact the dimer, see below) but for more clearly defined peaks due to higher crystallinity.

3.2. EQCM Analysis. The determination of the electron stoichiometry for the oxidative redox process of the polymer films was made with EQCM.[6] Thus deposits gave a ratio of reversible charge at full oxidation (at 0.9 V for (Me2T3S)2, (H2T3S)2, and H4BTA; 1.0 V for BTD) to dry weight (at the undoped state) corresponding to the passage of 2.0 F (repeat unit)$^{-1}$. This means that two electrons are given to form a bipolaron state, as usually observed in sexithiophenes.[6,7] The storage of two electrons per repeat unit is in agreement with an essential localization of the charge in the sexithiophene moieties, independently of the nature of the bridge connecting them.

In the case of H4BTE dimer deposits, the ratio of the reversible charge involved in the overall oxidative redox process (up to 0.85 V) to the stable dry mass corresponds to 4.0 electrons, i.e., the dimer behaves like a dodecathiophene chain.[7]

In situ EQCM analysis as a function of potential has been performed in the case of poly(BTD) as a typical case (Figure

(40) Zotti, G.; Martina, S.; Wegner, G.; Dieter, A. F. *Adv. Mater.* **1992**, *4*, 798.

(41) Hapiot, P.; Lagrost, C.; LeFloch, F.; Raoult, E.; Rault-Berthelot, J. *Chem. Mater.* **2005**, *17*, 2003.

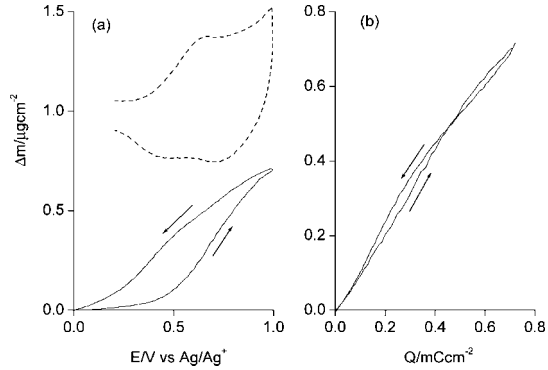

Figure 3. Mass change vs (a) potential and (b) redox charge for poly(BTD) in acetonitrile + 0.1 M Bu_4NClO_4. Dashed line: CV for comparison.

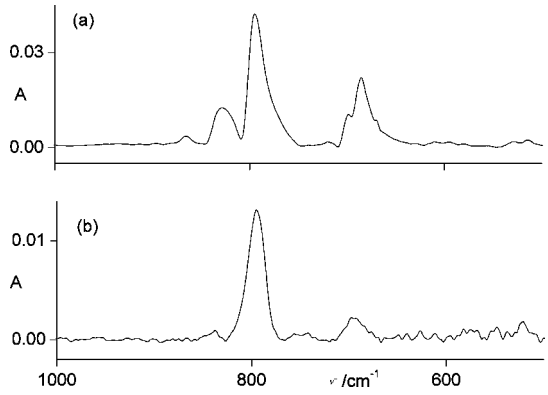

Figure 4. FTIR spectra of (a) BTA and (b) poly(BTA) films on platinum.

3). The mass of the polymer increases during oxidation and is reversibly decreased upon backward reduction. The increase is practically linear with redox charge and corresponds to a mass/charge ratio Fm/Q = 100, which indicates the reversible uptake of one perchlorate anion. Thus it is inferred that no solvation accompanies the process, as commonly observed in polythiophenes.[42]

3.3. FTIR Spectroscopy. FTIR spectroscopy has been used for a control of the regularity of coupling and to evaluate the degree of polymerization DP of the electrodeposited polymers that are insoluble in the common organic solvents.

According to a previous analysis,[9] the FTIR spectrum of the polymer from (T3CH2)2 shows two intense bands at 790 and 690 cm^{-1}, attributable to the C−H out-of-plane bending vibrations of 2,5-disubstituted and 2-substituted thiophene rings, respectively. A comparison of their absorption intensities $R = A_{690}/A_{790}$[43] indicates that the polymer is in fact the dimer. Similarly, the FTIR spectra of the poly(BTA) (Figure 4) and poly(BTE) films show an intensity ratio R decreased strongly compared with the monomer, giving the polymer a DP = 2.5 (dimer−trimer mixture) and 2 (dimer). Though relatively short, these polymer chains are anyway 12−18 rings long.

In poly(BTD), the spectrum is dominated by the band at 795 cm^{-1}, the end-ring band at 690 cm^{-1} being almost disappeared and the other bands in practice unchanged. Thus it results that the material is the expected α-coupled polymer with a high DP.

A slightly different analysis was of course applied to the substituted polymers. The FTIR spectrum of the polymer film from (Me2T3S)2 shows that among the bands at 831, 796, and 707 cm^{-1}, due to out-of-plane bending modes of the C−H bond in the inner, central, and terminal thiophene rings, respectively, the latter has decreased its intensity by ca. 10 times compared with that at 796 cm^{-1}, indicating that the polymer has a DP = ca. 10 (namely 60 thiophene rings). Similarly, in the case of poly(H4BTA), using the bands at 834, 792, and at 724 cm^{-1} allowed us to determine for the polymer a DP = 5 (30 thiophene rings).

The higher DP obtained for the substituted polymers is due to the higher solubility of the oligomers, which allows longer chains to be produced before precipitation on the electrode surface.

A different pattern is shown by the FTIR spectrum of H4BTE. In this case, the monomer film shows a strong band at 930 cm^{-1}, due to C−H out-of-plane bending modes of a double bond for a trans-dispositions of the T3 ends. Similarly, strong bands are shown at 834, 794, and 725 cm^{-1} and are due to modes of hydrogen atoms at the alkylsubstituted, the inner, and the terminal rings, respectively. The dimeric nature of the product of one-electron oxidation of H4BTE has been confirmed by the FTIR spectrum of the film compared with that of the monomer, showing that the band at 725 cm^{-1} has decreased its intensity by 50% compared with that at 930 cm^{-1}.

3.4. UV−vis Spectroscopy. The optical spectra of the polymer films electrodeposited on ITO and fully dedoped are displayed at maxima summarized in Table 1 along with the spectral maxima of the relevant monomers in solution.

The polymers from (Me2T3S)2 and (H2T3S)2 show a band at ca. 450 nm attributable to the coupled T6 moieties. The band is clearly red-shifted compared with that of the monomer, which appears at the same maximum of terthiophenes so that no electronic influence appears to be given by the disulfide bridge.

The optical spectrum of the yellow solution of BTD shows a maximum at 434 nm, i.e., very close to the maximum of sexithiophene at 432 nm (2.88 eV),[44] which indicates that the carbine moieties conjugate the two terthiophene moieties effectively. The optical spectrum of the poly(BTD) red film shows a maximum at 475 nm, i.e., the polymer displays a more extended degree of conjugation though the maximum is not much different from that of dodecathiophene (480 nm[39]). The latter result is not in contrast with the expectedly high DP because of the known saturation of conjugation at high DPs.[44a,45] The completely saturated point of the red-shift, defined as the effective conjugation length, is not much longer than 10−20 repeat units depending on the substituents.

The optical spectrum of BTA solution shows a maximum at ca. 400 nm, i.e., less close than BTD to the maximum of sexithiophene, which indicates that a single carbine moiety conjugates the two terthiophene moieties to a lesser extent

(42) Zotti, G.; Zecchin, S.; Schiavon, G.; Vercelli, B.; Berlin, A.; Dalcanale, E.; Groenendaal, L. *Chem. Mater.* **2003**, *15*, 4642.
(43) Furukawa, Y.; Akimoto, M.; Harada, I. *Synth. Met.* **1987**, *18*, 151.
(44) (a) Havinga, E. E.; Rotte, I.; Meijer, E. W.; Hoeve, W. T.; Wynberg, H. *Synth. Met.* **1991**, *43*, 473. (b) Chosrovian, H.; Rentsch, S.; Grebner, D.; Dahm, D. U.; Birckner, E.; Naarmann, H. *Synth. Met.* **1993**, *60*, 23.
(45) (a) ten Hoeve, W.; Wynberg, H.; Havinga, E. E.; Meijer, E. W. *J. Am. Chem. Soc.* **1991**, *113*, 5887. (b) Meier, H.; Stalmach, U.; Kolshorn, H. *Acta Polym.* **1997**, *48*, 379.

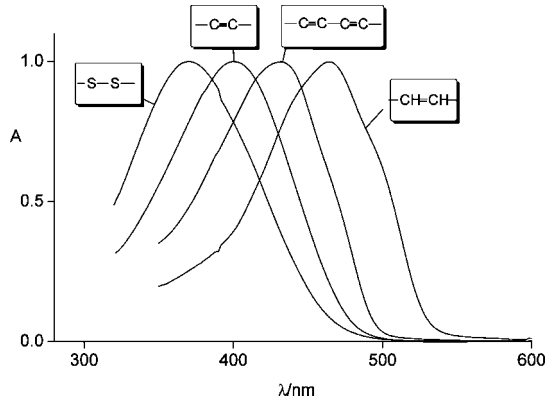

Figure 5. UV−vis normalized spectra of (from left) (Me2T3S)2, BTA, BTD, and BTE solutions.

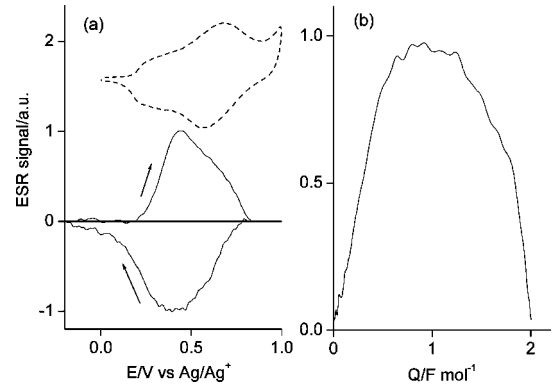

Figure 6. In situ ESR signal vs (a) potential and (b) charge of poly(Me2T3S)2 film in acetonitrile + 0.1 M Bu_4NClO_4 (the signal is inverted in the backward scan for clarity). Scan rate: 0.02 V s^{-1}. Dashed line: CV for comparison.

than two in sequence. Similar results are found in poly(BTA) compared with poly(BTD), whereas in poly(H4BTA), the maximum of the polymer film is red-shifted vs poly(BTA) from 450 to 474 nm.

The BTE solution in $CHCl_3$ shows a maximum at 465 nm (2.68 eV), i.e., the longest in the series of oligomers, which indicates that a single ethylene moiety conjugates the two terthiophene moieties in a very effective way. H4BTE shows its maximum at 440 nm, i.e., blue-shifted compared with BTE because of steric actions from the solvent-swollen hexyl substituents.

The poly(BTE) film shows a maximum at 500 nm for very thin films. Thicker films show a band blueshifted to 432 nm because of H-aggregate formation, together with the band at lower energy resulting in a red slope, as commonly found in crystalline oligothiophenes such as, for example, T6.[46] The H4BTE-dimer shows its maximum at 510 as thin film as in the case of poly(H4BTE) film, so that it is argued that the polymer is in fact the dimer. This result must be ascribed to the low reactivity to coupling of the radical cation of BTE and H4BTE, due to the efficient communication between the terminal terthiophene moieties through the ethylene bridge. This fact accounts also for the high conductivity of these materials.[14]

The discussed progression of conjugation is clearly evidenced in Figure 5 where the UV−vis normalized spectra of monomers (Me2T3S)2, BTA, BTD and BTE solutions are shown.

The relationship between conjugation and conduction will be clear later but it will also be evident that crucial is the comparison between triple and double bonds. For this reason the in vacuo optical properties of some oligomers were also theoretically investigated. To this end, the lowest-energy electronic excited states were calculated at the B3LYP/6−31G** level within the time-dependent DFT (TDDFT) approach for three model systems, i.e., T6, BTA, and BTE. T6 is the sexithiophene conjugated basis where one triple (BTA) or double (BTE) bond is inserted in the middle to modify conjugation.

TDDFT calculations predict for these chromophores the existence of one intense electronic transition in good agreement with experimental data even when the absorption spectra are recorded in solution, and deviations between the measured and calculated excitation energies were on the order of 0.5 eV. The intense absorption observed around 400−500 nm is assigned to the HOMO → LUMO one electron promotion calculated at around 2.3 eV (T6, 2.39 eV; BTA, 2.46 eV; BTE, 2.26 eV). Theoretical calculations slightly underestimate the energy of the bands. This underestimation can be due to the fact that B3LYP calculations predict almost planar structures for the oligothiophene backbone, and more twisted structures can be present in solution. Planar structures favor electron delocalization along the carbon−carbon conjugated path and narrows the HOMO−LUMO energy gap. Previous studies have shown that DFT calculations underestimate the twisting angle in oligothiophenes.[47]

However, the bathochromic shift of the λ_{max} value of BTE is well-reproduced by theoretical calculations (i.e., the excitation wavelength increases by 33 nm in CH_2Cl_2 solution from T6 to BTE and it is calculated to increase by 31.1 nm). Similarly, TDDFT qualitatively predicts the blue-shift of the lowest energy absorption band of BTA with respect to T6.

3.5. ESR Spectroscopy. Oxidation of the polymer films (with the exception of H4BTE-dimer, see below) produces an ESR signal that initially increases with charge, attains a maximum, and then decreases to zero at the two-electron (full) oxidation level (Figure 6). This is accounted for by the subsequent formation of the paramagnetic radical cation and of the diamagnetic dication. On the reverse scan, the signal reappears with a maximum in the intermediate potential range and at full back reduction the signal disappears completely. As a function of redox charge the signal attains its maximum at 50% doping charge, corresponding to 1 F (repeat unit)$^{-1}$ (Figure 6b).

Films of H4BTE dimer (Figure 7) show the appearance of a signal with a maximum intensity at the first redox potential, followed by a decrease, a second maximum at the second redox potential, and then a clear decrease at full four-electron oxidation. The maximum spin concentration is low

(46) Fichou, D.; Horowitz, G.; Xu, Z.; Garnier, F. *Synth. Met.* **1992**, *48*, 167.

(47) (a) Viruela, P. M.; Viruela, R.; Ortí, E.; Brédas, J.-L. *J. Am. Chem. Soc.* **1997**, *119*, 1360. (b) Casado, J.; Zgierski, M. Z.; Hicks, R. G.; Myles, J. T.; Viruela, P. M.; Ortí, E.; Ruiz Delgado, M. C.; Hernández, V.; López Navarrete, J. T. *J. Phys. Chem. C* **2005**, *109*, 11275.

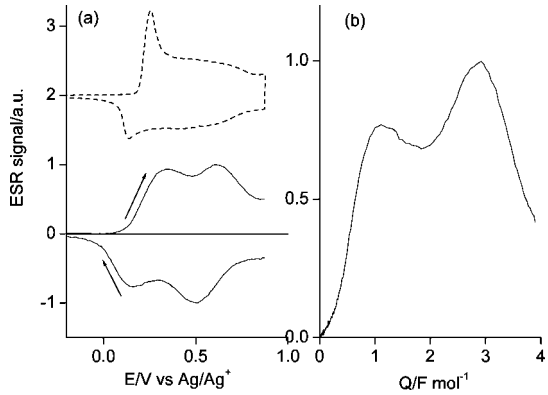

Figure 7. In situ ESR signal vs (a) potential and (b) charge of H4BTE dimer film in acetonitrile + 0.1 M Bu_4NClO_4 (the signal is inverted in the backward scan for clarity). Scan rate: 0.02 V s^{-1}. Dashed line: CV for comparison.

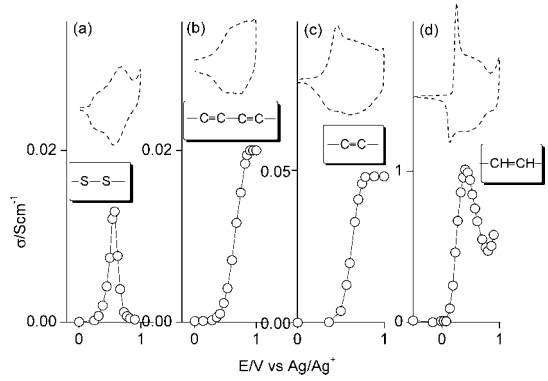

Figure 8. In situ conductivity vs potential of (a) poly(Me2T3S)2; (b) poly(BTD); (c) poly(H4BTA); (d) H4BTE dimer film in acetonitrile + 0.1 M Bu_4NClO_4. Dashed lines: CVs for comparison.

(0.04 spins mol^{-1}) as a consequence of the close proximity of the potentials of the two subsequent one-electron oxidation processes, which constitute each of the two two-electron processes. The persistence of spins at the anodic limit is attributable to Pauli paramagnetism of the metal-like conducting material.

3.6. Conductivity. Conductivity values of the investigated polymers are summarized in Table 1.

We have previously reported[9] that the in situ conductivity of poly((T3CH2)2) reaches a maximum of 5×10^{-3} S cm^{-1}, which is quite close to that (1×10^{-2} S cm^{-1}) of α,ω-dimethyl-capped T6.[5] The conductivity is redox-type at the radical-cation/dication couple as for isolated sexithiophenes.[5,6] An interchain hopping mechanism is forced by the interruption of conjugation by the aliphatic bridge.

The same results are obtained with the disulfide bridge. The conductivity of poly(Me2T3S)2 and poly(H2T3S)2 is also redox-type and gives a maximum of 2×10^{-2} S cm^{-1} and 1×10^{-2} S cm^{-1} for the methyl- and hexyl-homologues respectively (Figure 8a). The bridge is therefore not effective at all in favoring electron hopping between the connected T6 moieties.

The conductivity of poly(BTD) as a function of the applied potential (Figure 8b) shows a slope with conductivity approaching a value of 2×10^{-2} S cm^{-1} at 1.0 V. This result suggests that also in these carbine-connected sexithiophenes the conductivity proceeds almost without the help of the carbine links via a direct hopping between sexithiophene blocks of adjacent polymer chains. In any case, the presence of the bridge shows up in the plateau shape of the conductivity-potential curve, i.e., the conductivity is persistent at the two-electron oxidation (as a bipolaron-type conduction), whereas in the disulfides it drops to very low values.

The conductivity of poly(BTA) and poly(H4BTA) as a function of the applied potential (Figure 8c) is similar with the diacetylene case showing a sigmoid shape with a limit conductivity value of 2×10^{-2} and 5×10^{-2} S cm^{-1} respectively at full oxidation. Thus the conductivity of these carbine-connected sexithiophenes proceeds with a limited help of the carbine linker. The latter allows rotation along the molecular axis so that a free packing of the T6 moieties is allowed, though some communication through the bridge, which gives the CV characteristics of a fully conjugated polymer, allows a further conduction pathway and a moderately higher bipolaron-type conductivity.[7]

The conductivity of poly(BTE) could not be measured since films are too brittle but measurements could be made on H4BTE-dimer films cast on the conductivity electrode. Conductivity sets in with I_2-doping attaining a limit conductivity of 5 S cm^{-1}. The potential-driven conductivity as a function of the applied potential (Figure 8d) shows a peak shape with a maximum conductivity value of 1 S cm^{-1}, which decreases to ca. 50% at full oxidation. The maximum occurs at 50% of the full doping charge, in agreement with the recent results on a regular dodecathiophene.[7] Accordingly conduction appears to be carried by bipolarons. It is noteworthy that the conductivity of the polymer from bisdithienylethylene[15] is practically the same (5 S cm^{-1}), which suggests that the length of the oligothiophene moiety in the polymer chain is of lesser importance.

3.7. Polymers from T3, Me2T3, and H2T3. The polymers investigated in this report are better compared with the corresponding polymers without the bridge, namely, poly(T3), poly(Me2T3), and poly(H2T3) produced under the same conditions by anodic coupling of the corresponding terthiophenes shown in Scheme 2. Electrochemical, optical, and conductivity data are summarized in the lower section of Table 1.

As previously reported,[48] CV cycling of terthiophene T3 produces deposits of the dimer T6, which on prolonged CV cycling in the absence of T3 gives the α-coupled thiophene dodecamer (T12) through solid-state dimerization, as evidenced by electrochemical and UV−vis analysis.

Similarly, the monomers H2T3 and Me2T3 in acetonitrile show an irreversible oxidation process where potential cycling or potential step produce build-up of polymer. The electronic spectrum of poly(H2T3) (Figure 9a) upon CV cycling up to 0.8 V changes from a single peak at 433 nm (yellow film, essentially the dimer) to a broad and vibronically structured absorption with maximum at 532 nm (violet film). This results from solid-state polymerization by potential cycling through radical cation forms, as illustrated by the last stages of the transformation (Figure 9b) where a clear isosbestic point at 525 nm marks the regularity of the transformation. The CV of the solid-state polymerized

(48) Zotti, G.; Schiavon, G. *Synth. Met.* **1990**, *39*, 183.

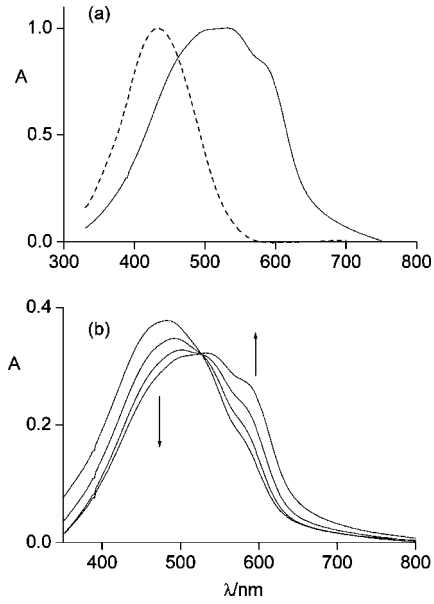

Figure 9. (a) UV−vis normalized spectra of poly(H2T3) film on ITO (- - -) before and (——) after solid-state polymerization. (b) Spectral evolution with progressive solid-state polymerization.

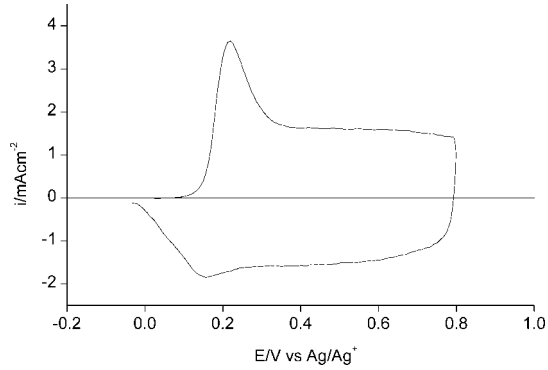

Figure 10. Cyclic voltammogram of poly(H2T3) film in acetonitrile + 0.1 M Bu_4NClO_4 after solid-state polymerization. Scan rate: 0.1 V s^{-1}.

poly(H2T3) film (Figure 10) shows a single redox process at $E^0 = 0.20$ V with a clear capacitive plateau. Analogous results are obtained for Me2T3.

From FTIR analysis of the bands at ca. 780 and ca. 710 cm^{-1}, poly(Me2T3) and poly(H2T3) films, electrochemically deposited and CV-cycled, result to have a DP = ca. 10 and 5, respectively (30 and 15 thiophene rings).

In situ conductivity of CV-conditioned deposits displays a plateau shape with a conductivity of 1 S cm^{-1} for poly(Me2T3), i.e., the same as that of poly(T3). In marked contras,t poly(H2T3) attains a conductivity of 50 S cm^{-1}. The UV−vis results evidence in fact a strong bathochromic effect of the hexyl substituents in the solid state, which is attributable to a specific coplanarizing and rigidifying effect of the hexyl substituents, not shown in the nonsubstituted polymer (507 nm) and in the methylsubstituted one (500 nm). As a matter of fact, the interactions among aliphatic chains are responsible for increased order and orientation of poly(3-alkylthiophene) chains and α,ω-oligothiophenes deposited onto a substrate. This effect is at the origin of the much higher conductivity of the hexyl-substituted polymer, similar to the behavior of regioregular poly(3-alkylthiophene)s by McCullough.[49]

3.8. Conduction in Sexithiophene Polymers.

3.8.1. Bridge. As recently found in OFETs based on regioregular poly(3-hexylthiophene), the orientation of the conjugated plane largely affects the overall mobility.[18] Two different orientations of the microcrystalline polymer domains with respect to the OFET substrate have been identified. Mobility is much higher (by 3 orders of magnitude) through polymer segments arranged in cofacial planes normally to the current flow, and charge transport is essentially blocked among segments lying on the same plane parallel to current direction.

Such hindrance may be overcome by the use of suitable bridges. A comparison between lateral (through-bridge) and parallel (face-to-face) conductivity for disulfide, diacetylene or acetylene and ethylene bridges can be made with the help of Scheme 3 as follows.

In the case of disulfide (B), the conjugation of the two sulfur atoms in the dication form with the thiophene rings could have given a lateral contribution to conduction. In fact the conductivity is the same as for a covalent ethane bridge (A). It is suggested that the different energy of the carbon and sulfur orbitals and their scarce overlapping (2p and 3p orbitals) is responsible for the failed enhancement of conduction.

We will then consider the diacetylene and acetylene bridges (C) in Scheme 3. The maximum conductivity in our triple-bond polymers is low, supporting previous findings on polymers of this type.[19f] This result may be due to localization of injected positive charges in the sexithiophene moieties, which act therefore as the redox centers of the polymer. Charge localization may be expected because the triple bond has a relatively strong electronwithdrawing ability.[17]

Finally the polymers from anodic coupling of bis-terthienyl-ethylene display a much higher conductivity (1−5 S cm^{-1}), comparable with that of bisdithienylethylene (5 S cm^{-1})[15] but also of homopolymers such as poly(T3) and poly(H2T3). It is therefore inferred that the double bond is a very efficient bridge, acting as an extension of the polyene chain in the oligothiophene sequences or even as a short between the sexithiophene moieties. The presence of 3-substituents as small as the methyl group does not cause any significant effect whereas the hexyl chain does even favor conduction rather than hinder charge transport.

3.8.2. Triple and Double Bonds. The polaron delocalization length, which is a primary determinant of the charge mobility in conjugated electronic materials, has been located in the 2−3 nm range in acetylene-, phenylenevinylene-, and aryleneethynylene-based polymers.[50] Moreover, ESR and photoinduced electron transfer measurements on ethyne-linked porphyrin oligomers[51] and polymers[52] indicate that they can

(49) McCullough, R. D.; Tristam-Nagle, S.; Williams, S. P.; Lowe, R. D.; Jayaraman, M. *J. Am. Chem. Soc.* **1993**, *115*, 4910.
(50) Kuroda, S.; Marumoto, K.; Ito, H.; Greenham, N. C.; Friend, R. H.; Shimoi, Y.; Abe, S. *Chem. Phys. Lett.* **2000**, *325*, 183.
(51) Susumu, K.; Frail, P. R.; Angiolillo, P. J.; Therien, M. J. *J. Am. Chem. Soc.* **2006**, *128*, 8380.
(52) Winters, M. U.; Dahlstedt, E.; Blades, H. E.; Wilson, C. J.; Frampton, M. J.; Anderson, H. L.; Albinsson, B. *J. Am. Chem. Soc.* **2007**, *129*, 4291.

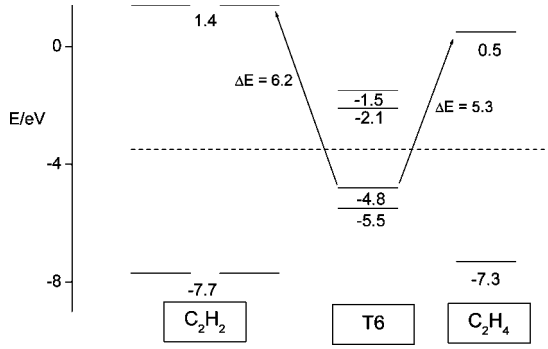

Figure 11. Energy level diagram of sexithiophene (T6), acetylene (C_2H_2), and ethylene (C_2H_4).

mediate essentially barrierless hole transport over distances of up to 7.5 nm.[51] Anyway, in our cases of polymers alternating sexithiophene and ethynylene moieties (type-C), compared with polymers in which a polyenic backbone is present (type-D), π-conjugation effects on the conductive properties are far less favorable.

The reason for this behavior may be recognized in the different electronic structure of the oxidized polymers. With ethynylene bridges the positive charges at the sexithiophene moieties yield bipolarons with a cumulene structure between the moieties shown in (C) in Scheme 3. This structure, differently from (D) in Scheme 3, is nonconjugated, which could make conductivity low.

Another possibility is a lower conjugation in type-C polymers. Raman and DFT analysis of Tn-diacetylene-Tn molecules ($n = 1-3$)[53] has clearly shown that triple-bond spacers in fact increase conjugation. Moreover, the rotation of the oligothienyl segments around the central diacetylenic bridge induces almost negligible changes both in bond distances and degree of conjugation, which is clearly attributable to the cylindrical symmetry of the diacetylenic spacer. These data confirm the ability of the triple bond to extend delocalization and rule out the suggested different conjugative effects on conduction between triple and double bonds.

A more satisfactory interpretation of the different conductive behavior appears to be one involving the energy gap between the sexithiophene moieties and the spacers. A similar alternation of energy levels can be in fact found in quantum wells based on polyacetylene-polydiacetylene copolymers.[54] To find a theoretical support to the suggested interpretation of the experimental results, we have carried out B3LYP/6−31G** calculations of the energies of the frontier molecular orbitals around the gap in three separate molecules: a chain of sexithiophene (T6) and two bridges, ethylene (C_2H_4) and acetylene (C_2H_2). The differences found between the HOMO of the oligothiophene and the corresponding LUMO of the bridges are, in the case of ethylene, 5.3 eV, whereas in the case of acetylene are 6.2 eV (see Figure 11). Thus, in a mechanism of hopping between two T6 chains through a separate moiety consisting of a double or a triple bond, there is roughly 1 eV difference in favor of hopping through an ethylenic link. In the actual chain, where such moieties are connected to the T6 sequences, the energy gaps given above are clearly lower, particularly between T6 and ethylene, but the qualitative picture is kept. In this connection we want to stress that the reason for the observed relative stability of the radical cation of bis-terthienyl-ethylene compared with bis-terthienyl-acetylene is right the fact that in the former case the unpaired electron is moving freely along the whole conjugated system, the central double bond constituting no appreciable barrier to intrachain transport.

The theoretical results given above, though strictly valid for the conduction in slightly doped molecules, could justify the higher values of conductivity found in heavily doped poly(bis-terthienyl-ethylene)s compared with poly(bis-terthienyl-acetylene)s.

Conclusions

Anodic coupling of bis-terthienyl-disulfide, -diacetylene, -acetylene, and -ethylene has produced electroactive polymer films on electrodes. The monomers are regularly coupled to polymers alternating sexithiophene sequences and bridge moieties of various conjugation.

The conductivities of p-doped poly(bis-terthienyl-disulfide)s are in practice the same as those of isolated or ethane-bridged sexithiophene, suggesting that conduction proceeds via a direct hopping between sexithiophene moieties of cofacial polymer chains.

Even with triple bond spacers (acetylene and diacetylene), which in any case effectively conjugate adjacent chains, conductivity does not increases appreciably. On the contrary, the simple double bond eases transport along the polyconjugated chains, presenting itself as the most efficient connection between coplanar sexithiophene moieties.

These conclusions may be helpful for the design of structures with efficient charge transport in organic electronic devices in general and for molecular electronics in particular. In conjugation with aromatic rings, double bonds may in fact be preferable to the triple bonds generally used for linear molecular wires such as phenylene-ethynylene oligomers.[55]

Acknowledgment. The authors thank Dr. G. Schiavon and Dr. S. Zecchin of the CNR for helpful discussions and S. Sitran of the CNR for his technical assistance. V.H. and J.T.L.N. are grateful to the MEC of Spain for the reseach project CTQ2006-14987-C02-01.

CM8023007

(53) Ruiz Delgado, M. C.; Casado, J.; Hernandez, V.; Lopez Navarrete, J. T.; Fuhrmann, G.; Bauerle, P. *J. Phys. Chem. B* **2004**, *108*, 3158.
(54) Ruckh, R.; Sigmund, E.; Kollmar, C.; Sixl, H. *J. Chem. Phys.* **1986**, *85*, 2797.
(55) (a) Fan, F. R.; Yang, J.; Cai, L.; Price, D. W.; Dirk, S. M.; Kosynkin, D. V.; Yao, Y.; Rawlett, A. M.; Tour, J. M.; Bard, A. J. *J. Am. Chem. Soc.* **2002**, *124*, 5550. (b) Kushmerick, J. G.; Naciri, J.; Yang, J. C.; Shashidhar, R. *Nano Lett.* **2003**, *3*, 897. (c) Pollack, S. K.; Naciri, J.; Mastrangelo, J.; Patterson, C. H.; Torres, J.; Moore, M.; Shashidhar, R.; Kushmerick, J. G. *Langmuir* **2004**, *20*, 1838. (d) Mayor, M.; Weber, H. B.; Reichert, J.; Elbing, M.; von Hänisch, C.; Beckmann, D.; Fischer, M. *Angew. Chem., Int. Ed.* **2003**, *42*, 5834. (e) Fan, F. R.; Lai, R. Y.; Cornil, J.; Karzazi, Y.; Brédas, J. L.; Cai, L.; Cheng, L.; Yao, Y.; Price, D. W.; Dirk, S. M.; Tour, J. M.; Bard, A. J. *J. Am. Chem. Soc.* **2004**, *126*, 2568.